



Short communication

## The neural networks based modeling of a polybenzimidazole-based polymer electrolyte membrane fuel cell: Effect of temperature

Justo Lobato<sup>a,\*</sup>, Pablo Cañizares<sup>a</sup>, Manuel A. Rodrigo<sup>a</sup>, José J. Linares<sup>a</sup>,  
Ciprian-George Piuleac<sup>b</sup>, Silvia Curteanu<sup>b</sup>

<sup>a</sup> Chemical Engineering Department, University of Castilla-La Mancha, Campus Universitario s/n. 13004, Ciudad Real, Spain

<sup>b</sup> Gh. Asachi Technical University Iasi, Department of Chemical Engineering, Bd. D. Mangeron, No. 71A, 700050 IASI, Romania

### ARTICLE INFO

#### Article history:

Received 3 October 2008

Received in revised form 23 January 2009

Accepted 23 January 2009

Available online 6 February 2009

#### Keywords:

PBI

PEMFC

High temperature

Neural network

Modeling

### ABSTRACT

Neural network models represent an important tool of Artificial Intelligence for fuel cell researchers in order to help them to elucidate the processes within the cells, by allowing optimization of materials, cells, stacks, and systems and support control systems. In this work three types of neural networks, that have as common characteristic the supervised learning control (Multilayer Perceptron, Generalized Feedforward Network and Jordan and Elman Network), have been designed to model the performance of a polybenzimidazole-polymer electrolyte membrane fuel cells operating upon a temperature range of 100–175 °C. The influence of temperature of two periods was studied: the temperature in the conditioning period and temperature when the fuel cell was operating. Three inputs variables: the conditioning temperature, the operating temperature and current density were taken into account in order to evaluate their influence upon the potential, the cathode resistance and the ohmic resistance. The Multilayer Perceptron model provides good predictions for different values of operating temperatures and potential and, hence, it is the best choice among the study models, recommended to investigate the influence of process variables of PEMFCs.

© 2009 Elsevier B.V. All rights reserved.

### 1. Introduction

Polymer electrolyte membrane fuel cells (PEMFCs) are receiving a growing interest for many potential power sources applications, both stationary and portable. The typical electrolyte membranes used in PEMFCs are Nafion or other perfluorcarbon sulphonic acid membranes. These have some limitations due to the presence of water required to be proton conductor and then, the temperature is limited to 90 °C at atmospheric pressure. Moreover, working above this temperature, the catalysts of PEMFCs are more tolerant to the presence of contaminants, overall higher operating temperature eliminates CO poisoning by eliminating CO occlusion of the platinum sites. In order to overcome this limitation, it has been proposed to raise the operating temperature [1–3]. This increase implies that all the materials used for this purpose must withstand those conditions (thermal stability), aside from having the adequate properties for their use in PEMFCs (e.g. proton conductivity for the polymeric membrane, catalytic activity for the electrocatalyst, chemical stability, mechanical stability, reliability, durability).

Polybenzimidazole (PBI), the polymer used in this work, can be included within the group of polymeric electrolytes proposed for High Temperature PEMFCs. When PBI is impregnated with phosphoric acid, it presents some interesting properties such as increasing of conductivity up to 200 °C which is acceptable and rising of thermal and chemical stability above the level. Thus, acid doped PBI can be used as polymeric electrolyte in High Temperature PEMFC [4–8]. A possible limitation of this system is the H<sub>3</sub>PO<sub>4</sub> stability within the PBI system, known as phosphoric acid is self-dehydrated and generates oligomers of the original acid, e.g., pyrophosphoric acid, at 140 °C [9] which leads to low conductivity [5]. Consequently, this undesirable process would produce a gradual decay of the cell performance. Thus, this process may degrade the cell performance along the time.

Detailed modeling of PEMFC has been of considerable interest in predicting the fuel cell performance and also for use in various systems engineering activities. Hence, there has been recent interest in building simply, cost reductive and time saving. Among the many possibilities, artificial neural networks (ANN) represent a good alternative choice [10].

The use of neural networks has become increasingly recommended for applications where the mechanistic description of the interdependence between variables is either unknown or very complex. Their parallel organization and their capability to learn from

\* Corresponding author. Tel.: +34 926 29 53 00x6707.  
E-mail address: [justo.lobato@uclm.es](mailto:justo.lobato@uclm.es) (J. Lobato).

the behavior of many chemical processes permit good solutions to problems where multiple constraints must be satisfied simultaneously, the high functionality and the rules are implicit than explicit.

Generally, there are some specific issues for neural networks which potential users should be aware of. Concerning the neural network modeling, some *advantages* can be mentioned. The neural networks have the capability to learn what happens in a process, without modeling the physical and chemical laws that govern the system. Consequently, they are very useful in approximation of any continuous nonlinear functions. The disadvantages seem to be upon the necessity in obtaining a perfect neural network with the experimental or operational history data. In other words, neural networks need large amount of good quality data for its training, which is normally difficult to obtain in practice. If they are properly trained and validated, the neural network models could be used to make accurate predictions on the process behavior, hence, leading to improve process optimization and control performance [11].

Neural network topologies are correlated with the nature of application and the type of the chemical system, e.g.: *feedforward* neural networks, for stationary conditions [12,13], *recurrent* neural networks, useful for long term predictions [14], *stacked* neural networks composed from some different or identical neural networks [15], *hybrid models*, which combine simplified phenomenological models with the neural ones [16,17], or neural network trained with *static and dynamic operating data* [18].

There are many reported studies about ANN modeling of fuel cells parameters based on simulated or experimental data [19–22]. Kumbur et al. [19] have used a feedforward error back propagation network based on four correlated input parameters (the non-wetting phase saturation, the compression pressure and the PTFE content of the DM (fuel cell diffusion media)) designed for one output (the capillary pressure). Rouss and Charon [20] have applied a multi-input and multi-output model implying one hidden multi-layer perceptron neural network combined with a time regression input vector approach for the mechanical nonlinear behavior of a proton exchange membrane fuel cell system with nine outputs. Saengrungs et al. [21] have studied and compared the performance predictions of a commercial proton exchange membrane (PEM) fuel cell system using two neural networks types: a back propagation with 2 hidden layers and a radial basis function networks—all of them based on two inputs (air flow and stack temperature) in order to determine the two outputs (stack voltage and stack current). In other case, Bao et al. [22] have implied a feedforward neural network for the air stream and hydrogen flow with recirculation in a PEM fuel cell system.

In this paper, a methodology based on simple neural networks with one single hidden layer was applied to study the performance of a polybenzimidazole-based PEMFC operating at high temperature, 100–175 °C. The influences of conditioning and operating temperatures and potential on the performance of the PEMFC were evaluated using three types of feedforward neural networks: Multilayer Perceptron (MLP), Generalized Feedforward Network (GFF) and Jordan Elman Network (JEN).

## 2. Experimental

### 2.1. Preparation of the membrane-electrode assemblies

In order to prepare the electrodes, it was followed the following procedure. On top of a gas diffusion media (Toray Graphite Paper, TGPH-120, 350 μm thick, 20% wet-proofed, ETEK Inc.), it was deposited by N<sub>2</sub>-spraying a micro-porous layer (MPL) consisting of 1 mg cm<sup>-2</sup> Vulcan XC-72R Carbon Black (Cabot Corp.) and 40% PTFE (Teflon™ Emulsion Solution, Electrochem Inc.). Next, it was

also N<sub>2</sub>-sprayed the catalyst layer, composed by Pt/C catalyst (20% Pt on carbon black, ETEK Inc.), PBI ionomer (5 wt.% PBI in N,N'-dimethylacetamide, DMAc) and DMAc as dispersing solvent. After depositing the catalyst layer, the electrodes were dried at 190 °C for 2 h. Afterwards, the electrodes were wetted with a solution of 10% H<sub>3</sub>PO<sub>4</sub> with a loading of 30 mg cm<sup>-2</sup>. Electrodes were left to absorb the acid overnight.

For the preparation of the MEA, a PBI membrane was taken out from an 80 wt.% phosphoric acid bath. Doping level acquired by the membrane was 6.5 molecules of acid per polymer repeating unit. The superficial acid onto the membrane was thoroughly wiped off with filter paper, and subsequently, it was used to prepare the MEA. In order to fabricate it, the doped membrane was sandwiched between a couple of electrodes, hot-pressing the whole system at 150 °C and 100 kg cm<sup>-2</sup> for 7 min. Once the MEA was ready, it was inserted into the cell. Active area of electrodes was 4.65 cm<sup>2</sup>.

### 2.2. Fuel cell tests

Cell hardware consisted of two bipolar plates made of graphite (Ralph Coidan, UK) into which it was machined channel with parallel geometry. Within the graphite plates, heating rods were fitted in order to heat the cell up. During the performed measurements, the cell was fed directly from the compressed bottles with pure hydrogen and oxygen at a flow rate of 0.2 l min<sup>-1</sup> and atmospheric pressure without any humidification system. It was used oxygen at high stoichiometry to avoid any diffusive limitation that would be boost with air [23] because the aim of this work was to study the pure temperature effects. Temperature was controlled with the aid of a temperature controller (CAL 3300, Cal Controls Ltd., UK).

The procedure to obtain polarization curves and impedance spectra can be depicted as follows. Firstly, the cell was kept at one temperature for 24 h, monitoring the current at a constant potential of 0.5 V. Afterwards, polarization curves and impedance spectra were consecutively recorded at the four temperatures used in this study, starting from the temperature in which the cell was conditioned and continuing from the lowest temperature to the highest one. Polarization curves were measured with a potentiostat/galvanostat. Unfortunately, this limited the upper limit of the current to 1 A, so that curves had to be stopped at a current density of 0.215 A cm<sup>-2</sup>. Once swept the four temperatures, the cell was again left for 24 h at the next temperature. The conditioning procedure was carried out from the lowest temperature (100 °C) up to the highest one (175 °C). Experiments were labeled as collected in Table 1. Impedance spectra were recorded by the Frequency Response Analyzer (FRA) Module of the potentiostat/galvanostat at a potential of 0.5 V. Frequency ranged from 10 kHz down to 10 mHz, with a potential wave of 0.05 V. In order to help to interpret the Nyquist plots corresponding to Impedance spectra the experimental data were fit to an equivalent circuit [24]. This consisted of a combination of an uncompensated resistance, accounting for the ohmic resistance of the system, with a parallel circuit containing a

**Table 1**  
Experimental data.

Conditioning temperature (°C)	Operating temperature (°C)	Label for experiment
100	100	P11
125	125	P22
150	150	P33
175	175	P44
125	100	P21
125	150	P23
125	175	P24
100	175	P14
150	175	P34

charge transfer resistance and a constant phase element related to the hydrogen oxidation, added in order to explain the small loop present at high frequency, and finally, another parallel circuit containing a new constant phase element and the polarization resistance for the oxygen reduction reaction (ORR). The appearance of a unique loop for the ORR impedes the distinction between the relative contributions of the charge transfer and diffusional processes, becoming both together in the polarization resistance. More information can be obtained from our previous work [24].

### 3. Process modeling

The transformation of a set of inputs into a set of outputs represents the main problem of a neural network modeling. The neural network model is obtained by *training* with input/output pairs, which have to be related by transformation which is being modeled. The adjustment of the neural network function to experimental data (learning process or training) is based on a nonlinear regression procedure. Training is done by assigning random weights to each neuron, evaluating the output of the network and calculating the error between the output of the network and the known results by means of an error or objective function. When the error becomes too large, the weights have to be adjusted and the process goes back for evaluate the output of the network. This cycle is repeated till the error becomes low or the convergence criterion is satisfied [25].

The main advantage of a neural network consists of the capacity of *generalization* (within limits) from these examples to other inputs that were not seen yet. As a general rule, the model is sought from experimentally available sets of data that clearly contain a number of very interesting relationships, feature correlations and other information which cannot be deduced in a straightforward manner from the first principles, by analytical solution or even with numerical methods. Many papers have been applied a multilayered, feedforward, fully connected network of perceptions because of its theory's simplicity, ease of programming and good results obtained. That is because its universal function in sense of network's topology has allowed to vary freely and it can take the shape of any broken curve [26].

In the present paper three types of neural networks that have as common characteristic the supervised learning control, i.e., MLP, GFF and JEN, has been used. MLP can approximate any input/output map, but they train slowly and require lots of training data. GFF networks are a generalization of MLP, the difference being into the connections that can jump over one or more layers. JEN networks supply the multilayer perceptron with context units, which are processing elements that remember past activity. Context units provide the network with the ability to extract temporal information from the data. In all three cases, the hyperbolic tangent axon (TanhAxon) transfer function was used [27]:

$$f = \frac{1 - e^{-2x}}{1 + e^{-2x}} \quad (1)$$

The training and validation of the neural models were performed with 16 series of experimental data obtained in our lab [23]. 10% of the whole set of data are kept for validation phase representing unseen data for the neural network. The neural networks designed for process under study have 3 input variables: conditioning temperature (Temperature 1, °C), the operating temperature (Temperature 2, °C) and potential (mV) and 3 outputs: the current density ( $\text{mA cm}^{-2}$ ), the cathode resistance ( $\Omega$ ) and the ohmic resistance ( $\text{m}\Omega$ ).

Many neural networks were trained and evaluated based on mean square error (MSE) and correlation ( $r$ )—the concordance between experimental data and neural network prediction. The

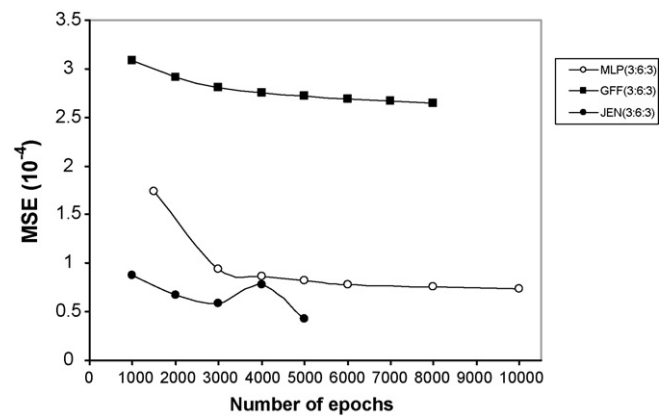


Fig. 1. The evolution of the MSE in the training process for the chosen neural models.

MSE was computed as:

$$\text{MSE} = \left( \sum_{j=1}^P \sum_{i=1}^N (d_{ij} - y_{ij})^2 \right) / (N \cdot P) \quad (2)$$

where:  $P$  is the number of output processing elements,  $N$  is the number of exemplars in the data set,  $y_{ij}$  is the network output for exemplar  $i$  at processing element  $j$ , and  $d_{ij}$  is the desired output for exemplar  $i$  at processing element  $j$ .

The best neural networks, which balance the size and the performance were: MLP (3:6:3) with  $\text{MSE}=0.0000737$ ,  $r=0.998$ , JEN (3:6:3) with  $\text{MSE}=0.00043$ ,  $r=0.9961$  and GFF (3:6:3) with  $\text{MSE}=0.00265$ ,  $r=0.9915$ . Fig. 1 presents the training process for these networks illustrated through the decrease of the MSE with the training cycles (epochs).

MLP (3:6:3) means a network of MLP type with 3 input neurons corresponding to the 3 input variables, one hidden layer with 6 neurons and 3 output neurons for the 3 output variables (Fig. 2).

### 4. Results and discussion

The performances of the three types of neural networks developed for the polymer electrolyte membrane fuel cell were evaluated comparatively.

The JEN (3:6:3) and GFF (3:6:3) present a higher training time and a lower efficiency comparatively to MLP (3:6:3). Consequently, the Multilayer Perceptron proves its universal character for approximation any continuous nonlinear function.

Fig. 3a and b present some examples for the decrease of the potential with current density obtained experimentally and predicted with MLP (3:6:3). They show that cell performances grow when temperatures increase from 100 to 150 °C. Thus, at 0.6 V, current densities are  $27.6 \text{ mA cm}^{-2}$  at 100 °C,  $31.6 \text{ mA cm}^{-2}$  at 125 °C,

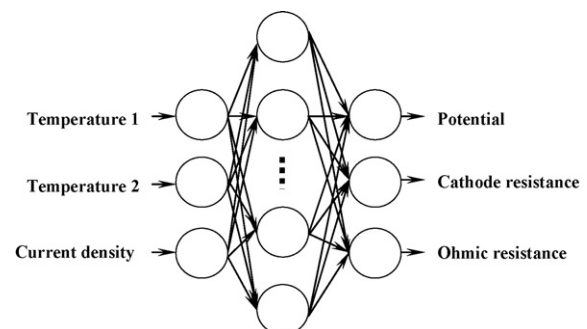


Fig. 2. The topology of the MLP (3:6:3).

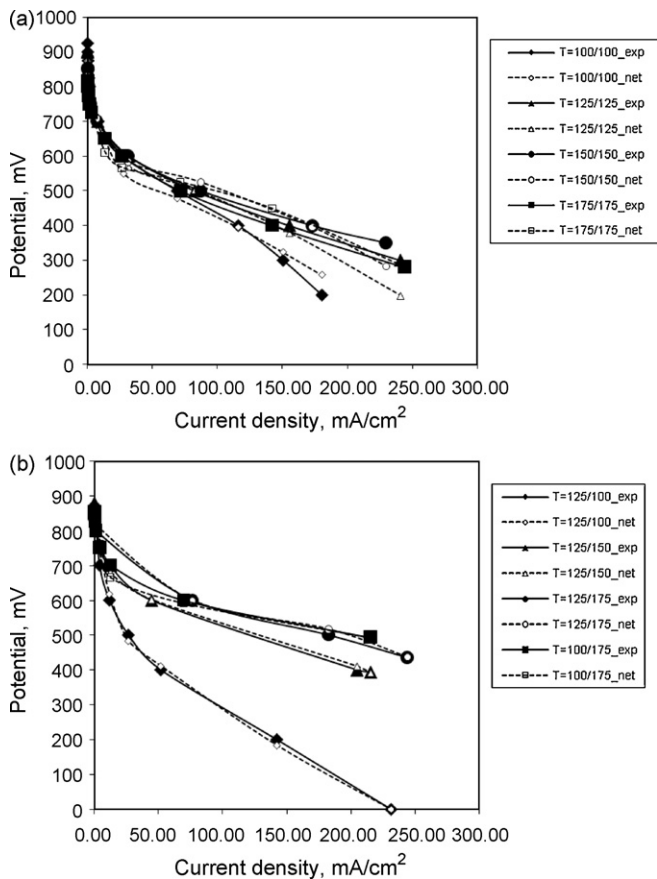


Fig. 3. Potential vs. current density obtained experimentally and predicted with MLP (3:6:3). (a) Conditioning temperature equal to operating temperature; (b) conditioning temperature different to operating temperature.

and 32.2 mA cm<sup>-2</sup> at 150 °C. However, at 175 °C, current density is 28.3 mA cm<sup>-2</sup>. In principle, it should be expected an increase of the cell performance as temperature goes up, as consequence of higher proton conductivity through the PBI membrane and enhanced electrodes kinetic. The notable increasing of the cell performance is observed at 100–125 °C, whereas the sensitively small increasing is presented at 125–150 °C. Also the performance decays are observed at 175 °C compared to the performance at 150 °C [24].

The neural model fits well the experimental data in the training stage. Therefore, the network learned well the behavior of the process.

In the validation stage the best prediction was reached by MLP network. Figs. 4–6 show the difference between the experimental data (cathode resistance, ohmic resistance and potential, respectively) and the predicted ones by the MLP model for nine examples.

It can be observed a good agreement between experimental and predicted data. Consequently the model could be applied to make supplementary predictions of the fuel cell process for working conditions which not belongs to experimental data set.

Very interesting results have been obtained from supplementary predictions. Different combinations of both temperatures between 100 to 120 °C for Temperature 1 (conditioning temperature) and 100 to 200 °C for Temperature 2 (operating temperature) were studied. In Table 2 the values for conditioning temperature (Temperature 1), operating temperature (Temperature 2), resistance, and current density are shown. The numbers 1–5 correspond to different combinations of temperatures where high power was observed. The numbers 6–9 contain experimental data in order to compare the power density obtained in different working conditions.

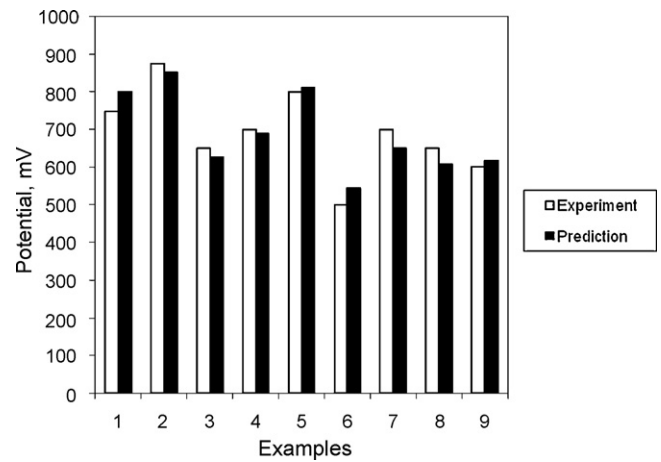


Fig. 4. Potential obtained experimentally and predicted by MLP (3:6:3) in the validation stage.

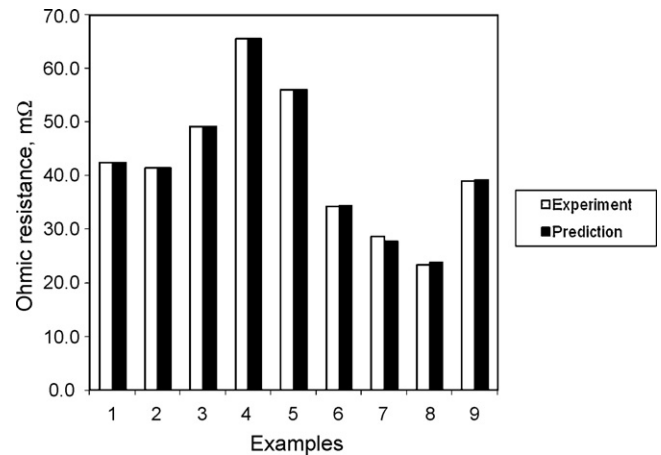


Fig. 5. Ohmic resistance obtained experimentally and predicted by MLP (3:6:3) in the validation stage.

Thus, it could be reached a peak power density over 90 mW cm<sup>-2</sup> approximately at intermediate operating temperature and low conditioning temperature. Higher values of operating temperature, 200 °C, do not lead to an improvement in the performance of the

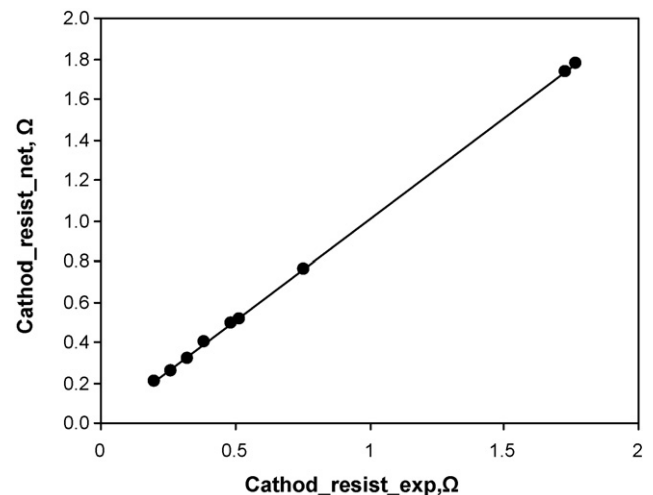
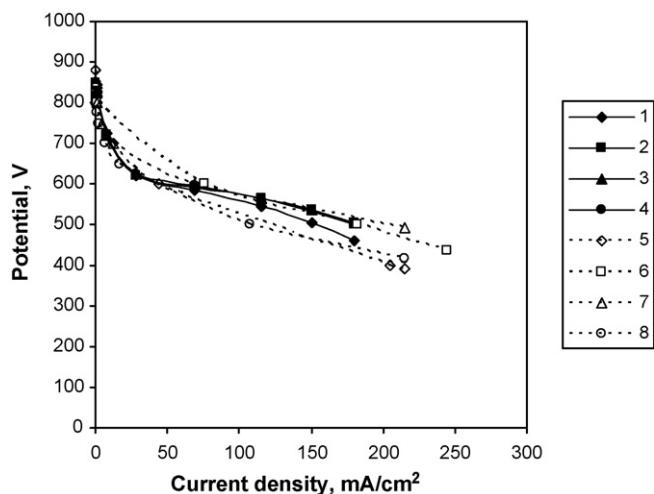


Fig. 6. Cathodic resistance obtained experimentally and predicted by MLP (3:6:3) in the validation stage.

**Table 2**  
Predictions obtained with MLP (3:6:3).

No.	Temperature 1 (°C)	Temperature 2 (°C)	Current density (mA cm <sup>-2</sup> )	Cathodic resistance (Ω cm <sup>2</sup> )	Ohmic resistance (mΩ cm <sup>2</sup> )	Potential (mV)	Power (mW cm <sup>-2</sup> )
1	120	150	180.4	1.81	153.9	460	82.92
2	100	160	180.4	1.30	123.2	505	91.17
3	105	160	180.4	1.35	127.4	503	90.69
4	110	160	180.4	1.39	131.6	499	90.09
5	110	200	116.0	0.74	103.7	568	65.92
6	125	150	215.0	1.81	159.0	394	84.73
7	125	175	244.1	1.25	133.0	435	106.18
8	100	175	215.0	0.93	108.3	493	106.02
9	150	175	215.0	1.49	181.3	418	89.90



**Fig. 7.** Potential vs. current density obtained with MLP (3:6:3) (1–4) and experimentally (5–8) (see Table 2).

fuel cell, as can be seen from the Fig. 7 and Table 2. The performance obtained in this work is not very high. Thus, Kongstein et al. reported 250 mW cm<sup>-2</sup> approximately at 125 °C but with 0.6 mg Pt loading on the cathode [28], Asensio and Gómez-Romero reported a peak power at 130 °C and humidified flows of 175 mW cm<sup>-2</sup> for a PBI-6.4 H<sub>3</sub>PO<sub>4</sub>, 100 μm thick and 165 mW cm<sup>-2</sup> approximately for a ABPBI-2.8 H<sub>3</sub>PO<sub>4</sub>, 70 μm thick [29]. But, it must be taking into account that the present work was carried out without an optimization of the different components of the MEA. Recent results in our lab have reached 550 mW cm<sup>-2</sup> approximately at 125 °C and 1.6 A cm<sup>-2</sup>. With respect to resistances, ohmic resistances of 200 mΩ cm<sup>2</sup> at 200 mA cm<sup>-2</sup> and 150 °C for a PBI-H<sub>3</sub>PO<sub>4</sub>, have been reported [30] or 120 for a commercial PBI-based MEA [31]. Polarization resistance of 0.28 Ω cm<sup>2</sup> at 200 mA cm<sup>-2</sup> and 160 °C has been also reported [31] but not information about the Pt loading used was given.

## 5. Conclusions

This work presents a methodology based on neural network modeling for an electrochemical process of a PBI-based fuel cell. Comparing the three types of neural model tested in this paper, we concluded that the MLP neural network showed the best correlation with experimental data, both in the training and validation steps. According with the predictions of the model and experimental data, the best performance of the power was at 150 °C for both studied temperatures (conditioning temperature and operating temperature).

The neural network modeling technique has as main characteristic to avoid the complex calculation of the modeling by mechanism and provides a basic guide for design and analysis of the PEMFC power systems and for the optimization of cell performance.

## Acknowledgements

The authors want to thank JCCM (Junta de Comunidades de Castilla-La Mancha) for the financial support for this research, through the project PBI08-0151-2045 and Mr. Piuleac wants also to thank SOCRATES-ERASMUS STUDENT MOBILITY.

## References

- [1] R. Savinell, E. Yeager, D. Tryk, U. Landau, J. Wainright, D. Weng, K. Lux, M. Litt, C. Rogers, *J. Electrochem. Soc.* 141 (1994) L46.
- [2] G. Alberti, M. Casciola, L. Massinelli, B. Bauer, *J. Membr. Sci.* 185 (2001) 73.
- [3] P. Costamagna, C. Yang, A.B. Bocarsly, S. Srinivasan, *Electrochim. Acta* 47 (2002) 1023.
- [4] J. Lobato, P. Cañizares, M.A. Rodrigo, J.J. Linares, G. Manjavacas, *J. Membr. Sci.* 280 (2006) 351.
- [5] J. Lobato, P. Cañizares, M.A. Rodrigo, J.J. Linares, J.A. Aguilar, *J. Membr. Sci.* 306 (2007) 47.
- [6] Q. Li, R. He, J.O. Jensen, N.J. Bjerrum, *Fuel Cells* 4 (2004) 147.
- [7] J.S. Wainright, M.H. Litt, R.F. Savinell, in: W. Vielstich, A. Lamm, H.A. Gasteiger (Eds.), *Handbook of Fuel Cells, Fundamentals, Technology and Applications*, vol. 3, John Wiley & Sons, New York, 2003, p. 436.
- [8] J. Lobato, M.A. Rodrigo, J.J. Linares, K. Scott, *J. Power Sources* 157 (2006) 284.
- [9] Y.-L. Ma, J.S. Wainright, M.H. Litt, R.F. Savinell, *J. Electrochem. Soc.* 151 (2004) A8.
- [10] W.-L. Lee, G.-G. Park, T.-H. Yang, Y.-G. Yoon, C.-S. Kim, *Int. J. Hydrogen Energy* 29 (2004) 961.
- [11] Z. Xiong, J. Zhang, *Chem. Eng. Proc.* 44 (2005) 477.
- [12] L.C. Wang, F.A. Wang, J.C. Song, S.L. Zhai, J.Q. Zhu, *J. Chem. Eng. Chin. Univ.* 18 (2004) 362–366.
- [13] S. Curteanu, *Central Eur. J. Chem.* 2 (2004) 113.
- [14] R.A. Aliev, R.R. Aliev, B. Guirimov, K. Uyar, *Appl. Soft Comput.* 8 (2008) 1252.
- [15] E. Llobet, P. Ivanov, X. Vilanova, J. Brezmes, J. Hubalek, K. Malysz, I. Gračia, C. Caneï, X. Correig, *Sens. Actuators B: Chem.* 96 (2003) 94.
- [16] O. Kahrs, W. Marquardt, *Comput. Chem. Eng.* 32 (2008) 694.
- [17] S. Curteanu, F. Leon, *Polym.-Plastics Technol. Eng.* 45 (2006) 1013.
- [18] I. Istadi, N.A.S. Amin, *Chem. Eng. Sci.* 62 (2007) 6568.
- [19] E.C. Kumbur, K.V. Sharp, M.M. Mench, *J. Power Sources* 176 (2008) 191.
- [20] V. Rouss, W. Charon, *J. Power Sources* 175 (2008) 1.
- [21] A. Saengrun, A. Abtahi, A. Zilouchian, *J. Power Sources* 172 (2007) 749.
- [22] C. Bao, M. Ouyang, B. Yi, *Int. J. Hydrogen Energy* 31 (2006) 1897.
- [23] J. Lobato, P. Cañizares, M.A. Rodrigo, C. Ruiz-López, J.J. Linares, *J. Appl. Electrochem.* 38 (2008) 793.
- [24] J. Lobato, P. Cañizares, M.A. Rodrigo, J.J. Linares, *Electrochim. Acta* 52 (2007) 3910.
- [25] M.P. Vega, E.L. Lima, J.C. Pinto, *Braz. J. Chem. Eng.* 17 (2000) 471.
- [26] F.A.N. Fernandes, L.M.F. Lona, *Braz. J. Chem. Eng.* 22 (2005) 323.
- [27] J.C. Principe, N.R. Euliano, W.C. Lefebvre, *Neural and Adaptive Systems: Fundamentals through Simulations with CD-Rom*, John Wiley & Sons, Inc., NY, 1999.
- [28] O.E. Kongstein, T. Berning, B. Borresen, F. Seland, R. Tunold, *Energy* 32 (2007) 418.
- [29] J.A. Asensio, P. Gómez-Romero, *Fuel Cells* 5 (2005) 336.
- [30] J.-H. Kim, H.-J. Kim, T.-H. Lim, H.-I. Lee, *J. Power Sources* 170 (2007) 275.
- [31] N.H. Jalani, M. Ramani, K. Ohlsson, S. Buelte, G. Pacifico, R. Pollard, R. Staudt, R. Datta, *J. Power Sources* 160 (2006) 1096.